INDONESIAN JOURNAL ON GEOSCIENCE
Geological Agency
Ministry of Energy and Mineral Resources

Journal homepage: http://ijog.geologi.esdm.go.id
ISSN 2355-9314, e-ISSN 2355-9306

# Geochemistry of Basaltic Merbabu Volcanic Rocks, Central Java, Indonesia

Sri Mulyaningsih[1] and Godang Shaban[2]

[1]Geological Engineering, Faculty of Mineral Technology, Institut Sains & Teknologi AKPRIND Yogyakarta
[2]Chemical Engineering, Industrial Technology, Institut Sains & Teknologi AKPRIND Yogyakarta

Corresponding author: sri_m@akprind.ac.id
Manuscript received: January, 31, 2018; revised: October, 23, 2018;
approved: December, 30, 2019; available online: June, 29, 2020

**Abstract** - The studied area is located along the hiking track of Kajor - Selo, the south flank of Merbabu Volcano, Central Java, Indonesia. Olivine basalt and augite-rich basalt compose the volcanic rocks. A geochemical study recognizes these basalts which tend to originate from the product of tholeiitic magma, in terms of transitional enriched mantle source. It is interpreted to have been formed as primary magma that mixed later with higher degrees of partial melting with a mantle wedge. Both fluid and melt were derived from the mixing of lower active continental margin and subducting oceanic slab. This study also shows general trends of increasing incompatible elements, *i.e.* Rb, Ba, $Pb^{2+}$, and Sr as LIL trace elements and Th, U, Nb, Ce, Zr, Hf, Nb, and Ta as HFS element comparing to basaltic andesites exposed at Thekelan, they show decreasing compatible of MgO, $Fe_2O_3$*, $Al_2O_3$, CaO, $TiO_2$, Ni, Sr, and Ba in line with increasing $SiO_2$. It was fractional crystallization process, shown by the slightly wide variation of Rb/Zr and La/Sm that indicates random crustal contamination.

**Keywords**: Merbabu, basaltic, geochemical, volcanic, magma, source



**How to cite this article:**
Mulyaningsih, S. and Shaban, G., 2020. Geochemistry of Basaltic Merbabu Volcanic Rocks, Central Java, Indonesia. *Indonesian Journal on Geoscience*, 7 (2), p.161-178. DOI: 10.17014/ijog.7.2.161-178

## Introduction

Merbabu Volcano is an active volcano in Central Java, Indonesia. It is located on the north of Merapi Volcano, the most active volcano in Indonesia (Figure 1). The last eruption of Merbabu Volcano was recorded in 1797 AD. Research on Merbabu volcanic activity, geology, magmatology, and others is very rare compared to research performed on Merapi Volcano. The recent researches on Merbabu Volcano discussed about volcano-stratigraphy (Mulyaningsih *et al*., 2016) and tectonic control (Mulyaningsih and Shaban, in press). Those researchers reported the lithology composing Merbabu Volcano that consisted of olivine-rich basalt (the oldest), basalt, and andesite (the youngest). This paper presents the whole-rock geochemistry of major, trace, and rare-earth element compositions for the basaltic volcanic rocks exposed along the hiking track of Kajor−Selo, in the southern flank of upper proximal facies. The aim of this study is to unravel its petrogenesis and tectonic setting of the eruptions. The results of this study complement the information available from other studies on the magmatism that affect the activity of Merbabu Volcano.

In the magmatic equilibrium system, magma is composed of minerals, silicate melt, and gases.

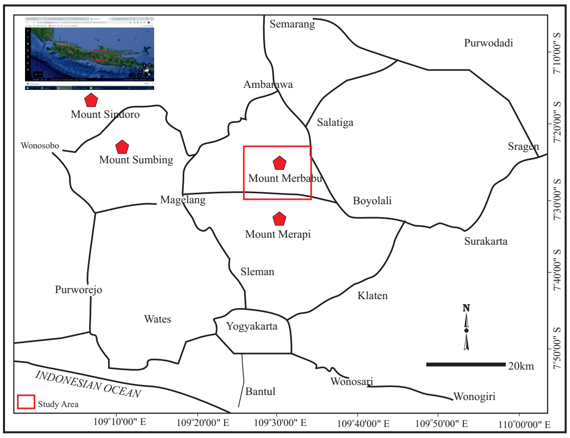


Figure 1. Index map of the studied area.

During its crystalization, compatible and incompatible elements were formed. The compatible elements are particularly partitioned into solid phases and the incompatible elements into melt phases (Winchester and Floyd, 1977). A previeous petrological study carried out by Mulyaningsih (2016) identified basalt and basaltic andesites composing lower part of Merbabu Volcano. By using compatible and incompatible elements containing within the basalt of Merbabu volcanic rocks, the magmatic characteristics of this volcano can be studied.

## Geological Setting

According to Hamilton (1979), Merbabu Volcano is located above the subducting zone of the Indian-Australian Plate (~ 10 km thick) under the Eurasian Plate (~20 km thick) as long as ~2,000 km, producing a trench as deep as 6 - 7 km and volcanic arc throughout Sumatra to Nusatenggara. Merbabu Volcano is one of the constituents of the volcanic arc. According to Bemmelen (1949), the volcanic chain in the study area is divided into two main volcanic paths, *i.e.* the northwest - southeast chain with Lawu-Merapi-Sumbing-Sindoro-Dieng Volcanos and the southwest - northeast chain with Merapi-Merbabu-Telomoyo-Ungaran-Muria Volcanos (Figure 2). The volcanic chains unidirectional with the main Central Java fault sistems aged Plio-Pleistocene, *i.e.* Semarang Fault and Solo Fault (van Bemmelen, 1949).

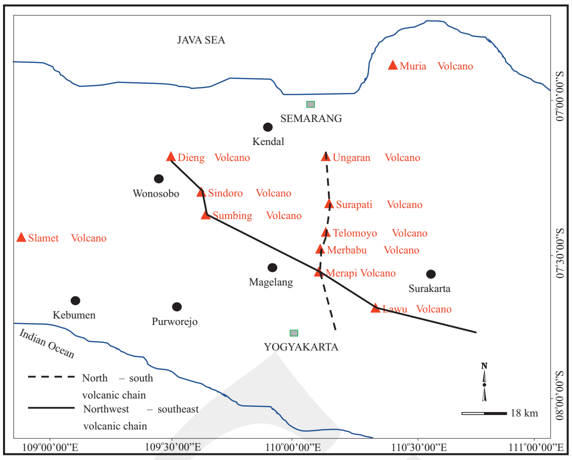


Figure 2. Main volcanic chains in Central Java; Merbabu Volcano forms the north-south path (source: Bemmelen, 1949 illustrated by Mulyaningsih, 2006).

As mentioned above, researches on Merbabu volcanism are very limited. Recently, an eruption has occured in a north northwest - south southeast fissure system that cut across the summit and fed the large-volume lava flows from Kopeng and Kajor craters on the northern and southern flanks, respectively (Anonim, 2013). An unconfirmed eruption might have occurred in 1570 (Mulyaningsih *et al.*, 2016). The 1797 eruption was explosive, rated 2 on the Volcanic Explosivity Index (Padang, 1951, in Anonim, 2013). It is widely known that Merbabu Volcano has been inactive for centuries since the last eruption in 1797 (Gomez, 2012).

## Sampling and Analytical Method

Twenty samples were taken from the surface outcrops, consisting of lava and dike, located along the sections of Thekelan and Kajor (Figure 3). Those samples were prepared for the laboratory work, including thin sections and rock powder for geochemistry. Thin section analyses were done using a polarizer microscope with 20x magnification at Petrology Laboratory IST AKPRIND Jogjakarta, Indonesia.

Twenty samples had been taken during the field work, but only eight representative samples from the distinguished suites were analyzed for

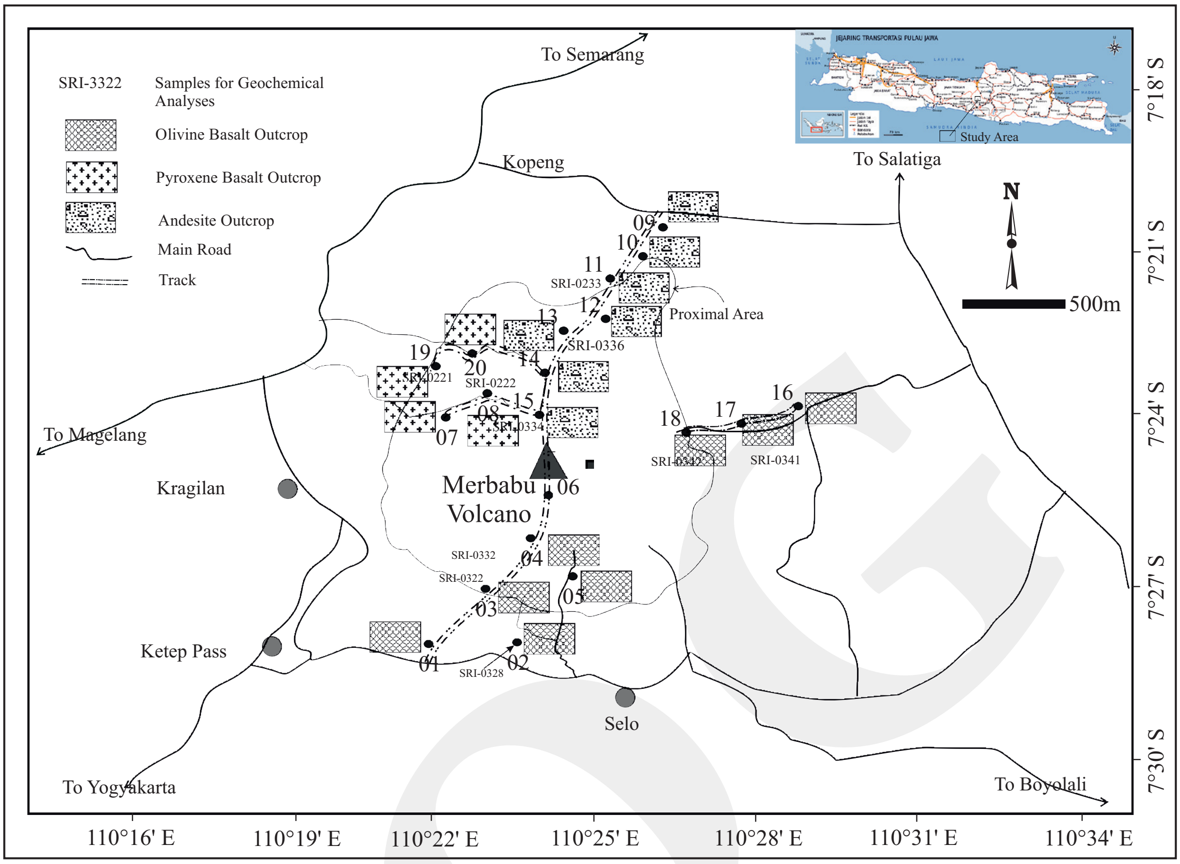


Figure 3. Track and sample locations, from Thekelan (north) and from Kajor (south).

major elements, and five samples for trace elements. The preparation were carried out in The INTERTEK Global Mineral Laboratory, Jakarta, Indonesia. The samples were pulverized into clay to silt sizes, then dried at 110°C. As much as 1g of dried powdered sample was then mixed with 7g of lithium metaborate, and fused in the furnace at 1,000°C for 10' so that it formed glass beads. It was then analyzed using X-ray Fluorescence Spectrometer (XRF). The loss of inignition (LOI) was counted by heating the samples at 1,010°C, then cooled until constant weight was achieved.

The trace element geochemistry can be explained as Mg numbers, calculated as $100\times Mg^{2+}/(Mg^{2+}+Fe_{total}^{2+})$. It is counted for the olivine basalts in the range of 99.973 to 99.974 (the elements presented on a water free basis). The trace elements were analyzed by mixing 0.25g of dried powdered sample with a flux of lithium metaborate and lithium tetraborate, then the mixture was fused in an induction furnace. The mixed sample was immediately poured into 5% $HNO_3$ (liquid), then stirred for ~30' until thoroughly dissoluted. An aliquot of the sample solution was spiked with internal In and Rh standards to cover the entire mass range and diluted 6,000 times prior to the introduction of ICP-MS for trace element analysis. The REEs were separated using conventional cation-exchange techniques.

## Results

### Petrology

The volcanic rocks of Merbabu Volcano outcropping along the tracks of Kajor - Selo represent mafic to intermediate compositional continuum as indicated by the range of colour, *i.e.* dark grey and very dark grey. Some outcrops consist of intersections of pyroclastic breccias (and tuffs), dikes, and dominantly by lavas. There are eight layers of olivine basaltic lavas exposed along the track of Kajor. Each layer consists of massive lava (50 - 90 cm thick), blocky lava, and (often) scoria lava. As a comparison, data were also collected along the hiking track of Thekelan through Selo. From the bottom to the top, there were a layer of olivine-rich basaltic lava, three layers of pyroxene-rich basaltic lava, and three or four sequences of andesitic volcanic materials (including breccia, lava, and tuff).

The olivine-rich basaltic lava exposed at Jrakah (below Kajor) has an age of 42.000± 100 ka by K/Ar (Mulyaningsih, 2006). The lava is characterized by very dark grey colour, vesicular, poikilitic, and composed of large phenocrysts of olivine, bytownite-labradorite, and augite embedded within the groundmass of glass and small crystals of olivine and plagioclase (Figures 4 and 5). Other olivine-rich basalts occur about 500 m east of Kajor (upper Jrakah) intersecting with Old Merapi volcanic materials. Megascopically, they are very difficult to distinguish. Based on the outcrop exposed on the middle flank of Bibi Volcano (Older Merapi), basaltic lava derived from Merapi Volcano is characterized by very dark colour, deeply weathered (forming very thick soils), porphyritic, and composed of olivine, augite, hypersthene, and labradorite. Geomorphologically, it is sourced from the southwestern side. The mineral grains of olivine-rich basalts coming from Merbabu Volcano are bigger with more euhedral shape, but have much smaller crystals and glasses, less massive, and less thicker than Merapi materials.

Further observations as comparison, outcrops in stop sites No. 9 - 11 with three steps of hummocky geomorphology, consist of layers of olivine-rich basalts (composing the base of valleys) overlain by pyroxene-rich basalt and

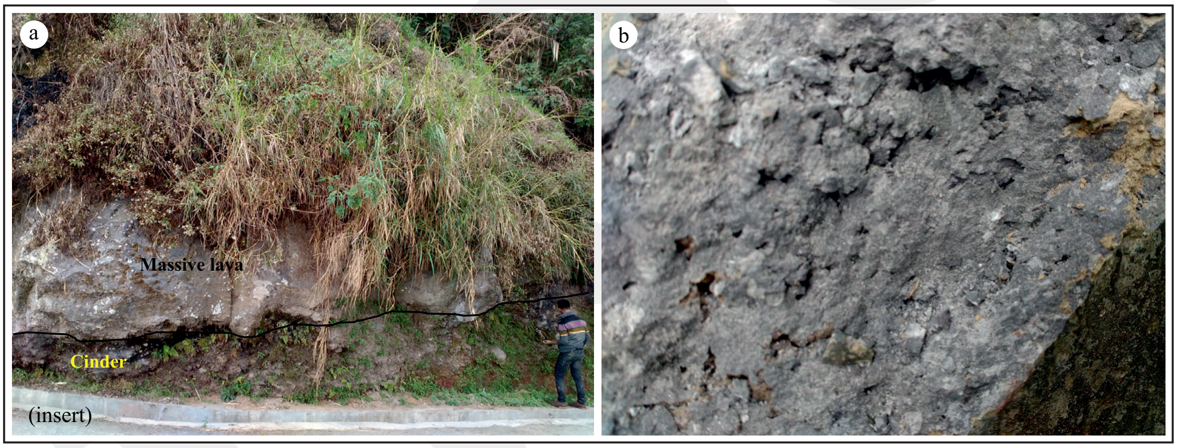


Figure 4. Field photographs of outcrops of olivine-rich basalt exposed at lower Kajor (a) and at Jrakah (b).

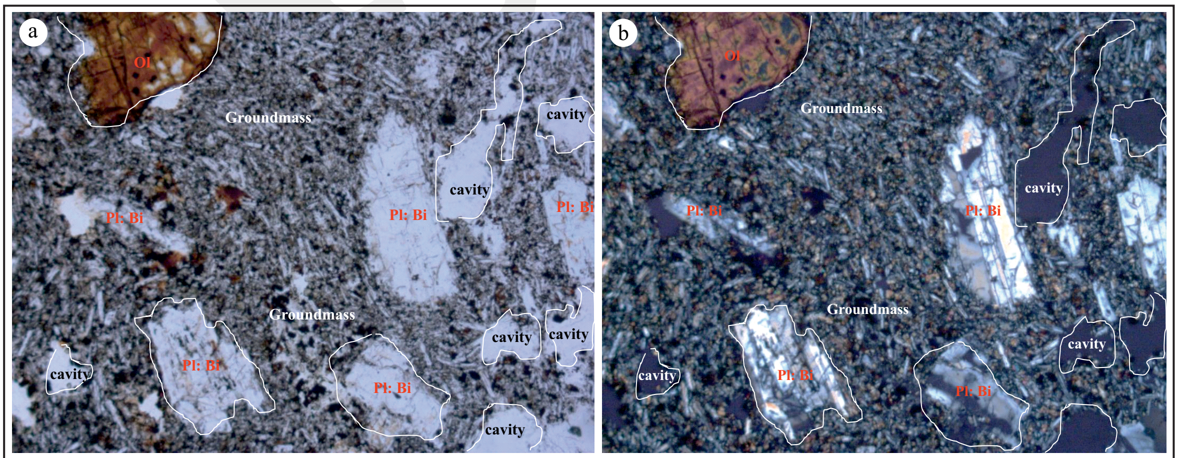


Figure 5. Photomicrographs of thin section of olivine-rich basalt exposed at lower Kajor, (a). parallel nicol, (b). ross nicol.

andesitic volcanic materials. The hummocks are separated by two valleys composed of intersectings of pyroclastic breccias, lavas, and tuffs. The lowest hummock that lies on the lava layers of olivine-riched basalt, consists of brecciated lava (± 40 cm thick), massive lava (± 60 - 80 cm thick) (Figure 6), and unsorted pyroclastic breccias. Other hummocks (stop cites No. 10 - 11) consist of collumnar-jointed lava (bottom), entablated lava (middle), and blocky lava (top), which is cut by a normal fault, forming steep Kedungkayang water fall as high as


Figure 6. Outcrops of basaltic - andesite lava exposed at Tegalrejo (stop site 19) upper Banyudono (a); close up of the basaltic lava (b); basaltic-andesite exposed at stop site 20, Banyudono(c)); close up of basaltic-andesite exposed at Banyudono (d); Photomicrographs of basaltic-andesite exposed at Banyudono: parallel nicol (e) and cross nicol (f).

~50 m. Those lava layers form the foot wall of waterfall, while other pyroclastic breccias and tuffs compose the hanging wall. The pyroxene-rich basalt (dark grey colour) is characterized by vesicular to massive, poikilitic-porphyritic, subhedral-anhedral natures, and composed of large grains of labradorite-bytownite, augite, and (rarely) olivine embedded within groundmass of glass and small crystals of mostly pyroxene and olivine (Figures 6e and f). Thus, it can be explained from the bottom to the top of the northern flank, from Kopeng to Thekelan, that it consits of intersections of pyroclastic breccias and massive lavas overlying olivine-riched basaltic and pyroxene-riched basaltic lavas. The middle track comprises hornblende-rich andesitic lavas overlain by three thin layers of orange lapilli (could be sourced from younger Merbabu or Sumbing Volcanoes). The upper section is dominated by very thick collumnar-jointed andesitic lavas (± 5 - 20 m) and dykes (stop sites No. 14 and 15). Some andesitic lavas are altered forming orange to white milk colour in the top. The andesite is vesicular, porphyritic, and composed of phenocrysts of andesine, hornblende, and augite (sometimes aegirine) within the groundmass of glasses (Figure 7). Some volcanic phenomena, such as mud pools, hot springs, and hot dry rocks are well identified. Near the summit, an irregular contact is also exposed between andesitic lava and olivine-rich basaltic lava.

## Major Elements

Volcanic rock classification can be divided based on the range contents of $SiO_2$ (silica contents) and total ($Na_2O$+$K_2O$). Olivine-rich basalt has silica contents ranging from 45 - 52%, basalt of 52 - 57%, and andesite has 57 - 63% (Figure 8;


Figure 7. Andesite lava exposed at Thekelan (stopsite 13): (a) the outcrop condition, (b) close up of the andesite, (c) its parallel nicol photomicrograph, and (d) its cross nicol photomicrograph.

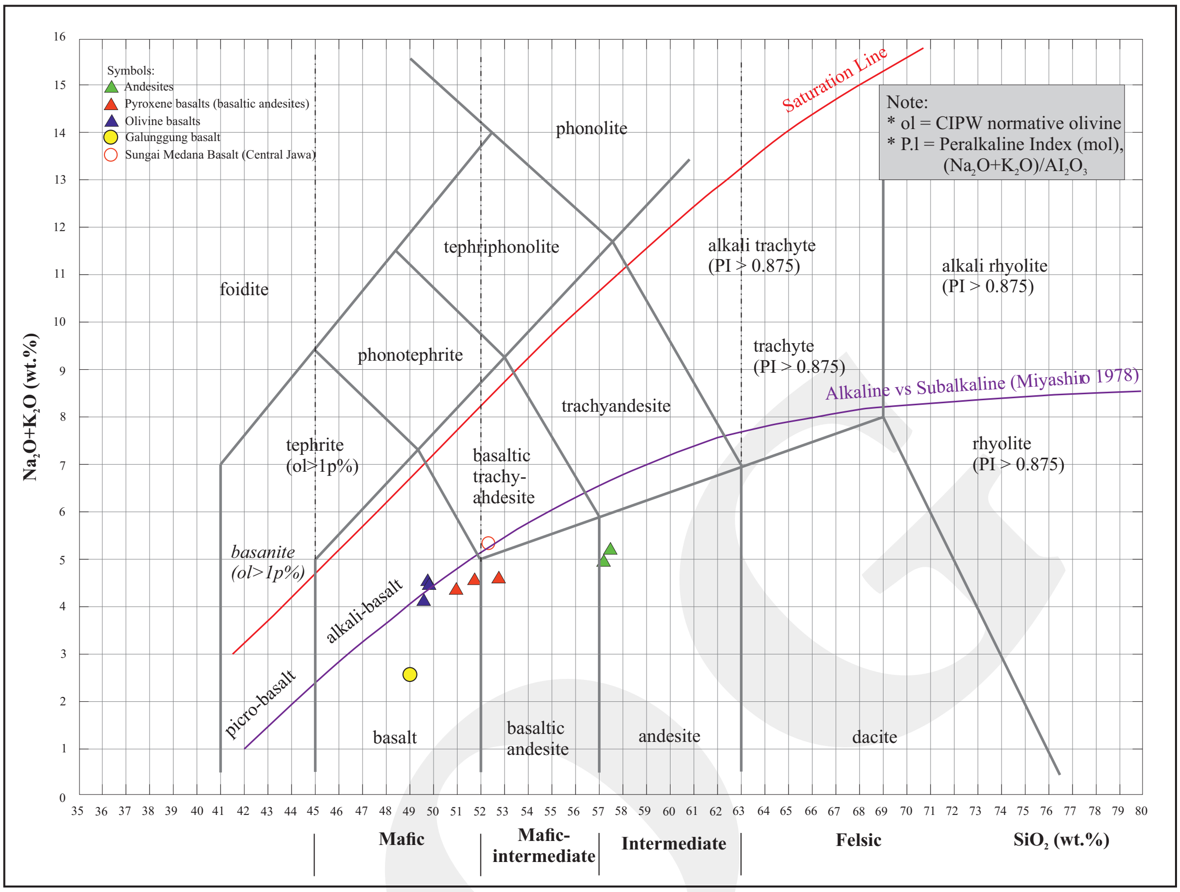


Figure 8. Total Alkali-Silica (TAS) classification schemes for Merbabu volcanic rocks, Medana River in Karangsambung (Anshori, 2007), and Galunggung volcanic rocks (Demsey, 2013, after Le Bas *et al*., 1986).

after Le Maitre, 2002; after Le Bas *et al*., 1986). The eight samples (of twenty thin sections) of olivine-rich basalt, basalt, and andesite were identified their major and tracs elements presented in Table 1. The silica contents range from 49 - 58 wt.%, indicating a wide range classification from mafic to intermediate volcanic series. Olivine-rich basalt has $SiO_2$ ranging from 49 - 50 wt.%, $TiO_2$= 0.82 - 0.84 wt.%, $Fe_2O_3$= 10.11 - 10.86 wt.%, MgO= 4.28 - 4.53 wt.%, and CaO (9.72 - 10.51). Merbabu basalt has $SiO_2$ range of 51 - 52.78 wt.%, $TiO_2$= 0.77 - 0.78 wt.%, $Fe_2O_3$= 8.88 - 9.99 wt.%, MgO= 3.01 - 3.88 wt.%, and CaO= 7.99 - 8.22 wt.%. TAS diagram (Total Alkali *versus* Silica) identifies olivine-rich basalt as basalt and pyroxene-rich basalt as basaltic andesite (Figure 8). As a comparison, Figure 9 is trapezoidal diagram presenting the total alkali/alumina *versus* $Na_2O/Al_2O_3$ according to Shands (1927). Merbabu basalt and basaltic andesite are shown as a potassic calc-alcaline volcanic series. In the next part, the olivine-rich basalt is called basalt, and the pyroxene-rich basalt is called basaltic andesite.

Compared to tholeiitic basalt of Galunggung Volcano in West Java (Demsey, 2013) and Medana River in Kebumen (Anshori, 2007) which were described as sodic calc-alkaline series, basalts of Merbabu Volcano are described as potassic calc-alkaline series (Figures 9). Other major element contents are presented in Table 1. Large grains of olivine are not common in the basaltic andesite volcanic rocks since the mafic minerals are dominated by augite-aegirine and little grains of olivine and pyroxene minerals. Compared to basaltic andesites of Galunggung volcanic rocks, the $SiO_2$ contents are ~54 - 56.79%, $Fe_2O_3$ of ~7 - 8.47%, higher in $Na_2O$ but lower in $K_2O$ than

Table 1. Major Elements (in wt.%) of Selected Olivine Basalt (SRI-0328 (bottom), SRI-0322 (middle) and SRI-0332 (top) Compared to Tholeiitic Basalt of Medana River, Karangsambung (Anshori, 2007) and Tholeiitic Basalt of Galunggung Volcano (Demsey, 2013), Basaltic Andesites: SRI-0221 (bottom), SRI-0222 (middle) and SRI-0233 (top) Compared to Basaltic Andesite of Galunggung Volcano (Demsey, 2013) and Andesite SRI-0336 (bottom) and SRI-0334 (middle) Compared to Basaltic and Andesitic Volcanic Rocks from Sumbing Volcano (Demsey, 2013)

| | Olivine Basalt of Merbabu Volcano | | | Tholeiitic Basalt of Karang-sambung (Anshori, 2007) | Tholeiitic Basalt of Galunggung Volcano Demsey, 2013) | | Basaltic Andesite of Galunggung Volcano (Demsey, 2013) | | | | | | Basaltic Andesite of Merbabu Volcano | | | | |
|---|---|---|---|---|---|---|---|---|---|---|---|---|---|---|---|---|---|
| | **SRI-0328** | **SRI-0322** | **SRI-0332** | **River Medana** | **Gal 132a** | **Gal 132b** | **Gal 133** | **Gal 134** | **Gal 135** | **Gal 136** | **Gal 137a** | **Gal 137b** | **SRI-0221** | **SRI-0222** | **SRI-0233** | **SRI-0336** | **SRI-0334** |
| *Major elements* | | | | | | | | | | | | | | | | | |
| $SiO_2$ | 49.60 | 49.80 | 49.85 | 52.35 | 49.1 | 49.06 | 56.27 | 56.79 | 55.99 | 55.98 | 54.77 | 54.58 | 51.02 | 51.77 | 52.78 | 57.25 | 57.45 |
| $TiO_2$ | 0.83 | 0.82 | 0.84 | 1.21 | 0.83 | 0.84 | 0.89 | 0.71 | 0.74 | 0.74 | 0.84 | 0.84 | 0.77 | 0.78 | 0.77 | 0.75 | 0.77 |
| $Al_2O_3$ | 19.91 | 18.86 | 19.34 | 15.09 | 15.93 | 15.93 | 19.87 | 18.22 | 18.73 | 17.88 | 18.94 | 18.95 | 20.01 | 18.44 | 19.19 | 20.22 | 18.23 |
| $Fe_2O_3$ | 10.11 | 10.89 | 10.14 | 10.33 | 10.32 | 10.18 | 7.47 | 7.74 | 8.13 | 8.17 | 8.35 | 8.47 | 9.91 | 9.99 | 8.88 | 7.14 | 8.07 |
| *MnO* | 0.17 | 0.17 | 0.18 | 0.14 | 0.17 | 0.17 | 0.14 | 0.16 | 0.17 | 0.16 | 0.15 | 0.14 | 0.18 | 0.18 | 0.17 | 0.18 | 0.15 |
| *MgO* | 4.28 | 4.32 | 4.53 | 3.03 | 10.33 | 10.14 | 2.35 | 3.62 | 3.57 | 4.35 | 4.31 | 4.30 | 3.88 | 3.55 | 3.01 | 2.07 | 2.48 |
| *CaO* | 10.51 | 9.72 | 10.07 | 7.01 | 11.19 | 11.15 | 8.09 | 7.99 | 8.23 | 8.36 | 8.63 | 8.66 | 8.19 | 7.99 | 8.22 | 5.81 | 6.66 |
| $Na_2O$ | 2.81 | 2.69 | 2.84 | 3.11 | 2.23 | 2.19 | 4.04 | 3.64 | 3.72 | 3.49 | 3.66 | 3.67 | 2.81 | 3.02 | 3.06 | 3.42 | 3.51 |
| $K_2O$ | 1.74 | 1.44 | 1.62 | 2.22 | 0.36 | 0.36 | 0.81 | 0.77 | 0.73 | 0.73 | 0.54 | 0.60 | 1.57 | 1.55 | 1.56 | 1.53 | 1.69 |
| *LOI* | 0.20 | 0.50 | 0.10 | 3.89 | 0.51 | 0.49 | 0.26 | 0.16 | 0.40 | 0.27 | 0.13 | 0.17 | 0.26 | 0.27 | 0.23 | 1.80 | 0.80 |
| $P_2O_5$ | 0.21 | 0.24 | 0.23 | 0.36 | 0.10 | 0.10 | 0.22 | 0.16 | 0.17 | 0.15 | 0.16 | 0.16 | 0.76 | 1.0 | 0.9 | 0.34 | 0.30 |
| *Total* | 100.23 | 99.55 | 99.77 | 98.73 | 100.09 | 99.63 | 99.89 | 99.64 | 99.78 | 99.74 | 100.22 | 100.20 | 99.36 | 98.54 | 98.77 | 100.51 | 100.11 |

Table 1. Continued....

| | Olivine Basalt of Merbabu Volcano | | | Tholeiitic Basalt of Karang-sambung (Anshori, 2007) | Tholeiitic Basalt of Galunggung Volcano Demsey, 2013) | | Basaltic Andesite of Galunggung Volcano (Demsey, 2013) | | | | | | Basaltic Andesite of Merbabu Volcano | | | | |
|---|---|---|---|---|---|---|---|---|---|---|---|---|---|---|---|---|---|
| | SRI-0328 | SRI-0322 | SRI-0332 | River Medana | Gal 132a | Gal 132b | Gal 133 | Gal 134 | Gal 135 | Gal 136 | Gal 137a | Gal 137b | SRI-0221 | SRI-0222 | SRI-0233 | SRI-0336 | SRI-0334 |
| *Trace elements* | | | | | | | | | | | | | | | | | |
| *K* | 14700 | 12400 | 13800 | | | | | | | | | | | | | 14300 | 12700 |
| *Cr* | 28.00 | 37.00 | 36.00 | <20.00 | 541.00 | 521.50 | 5.70 | 35.20 | 9.80 | 70.30 | 25.40 | 25.40 | | | | 6.00 | 6.00 |
| *Ni* | 21.00 | 25.00 | 27.00 | <20.00 | 163.10 | 157.80 | 5.70 | 14.40 | 8.20 | 25 | 14.90 | 16.10 | | | | 6.00 | 4.00 |
| *Co* | 30.00 | 28.00 | 29.00 | 26.00 | | | | | | | | | | | | 12.00 | 8.00 |
| *V* | 296.0 | 262.0 | 302.0 | 277.00 | 269.30 | 265.60 | 139.00 | 148.10 | 152.60 | 162.10 | 177.10 | 178.40 | | | | 141 | 92.00 |
| *Pb* | 15.00 | 18.00 | 18.00 | 25.00 | 3.80 | 3.90 | 6.70 | 6.80 | 6.50 | 6.50 | 4.50 | 5.30 | | | | 13.00 | 19.00 |
| *Zn* | 96.00 | 92.00 | 91.00 | 99.00 | | | | | | | | | | | | 99.00 | 106 |
| *Rb* | 23.70 | 22.10 | 23.10 | 49.00 | 7.50 | 7.50 | 18.10 | 18.20 | 16.10 | 17.70 | 12.50 | 10.00 | | | | 23.6 | 22.8 |
| *Ba* | 571.0 | 574.0 | 577.0 | 440.00 | 85.20 | 88.10 | 186.70 | 186.00 | 186.00 | 175.60 | 147.70 | 148.10 | | | | 380 | 585 |
| *Sr* | 549.0 | 602.0 | 593.0 | 267.00 | 208.20 | 207.40 | 284.10 | 266.10 | 275.10 | 259.60 | 277.10 | 279.00 | | | | 498 | 494 |
| *Ga* | 19.90 | 20.30 | 20.30 | 20.50 | 22.70 | | | | | | | | | | | 20.50 | 22.70 |
| *Cs* | 2.00 | 2.40 | 1.10 | 2.80 | 2.30 | | | | | | | | | | | 2.80 | 2.30 |
| *Nb* | 2.80 | 2.70 | 2.60 | 267.00 | 208.20 | 207.40 | 284.10 | 266.10 | 275.10 | 259.60 | 277.10 | 279.00 | | | | 5.50 | 7.30 |
| *Zr* | 53.30 | 58.20 | 59.20 | 142.00 | 46.00 | 46.50 | 125.00 | 91.20 | 86.40 | 85.90 | 101.30 | 102.00 | | | | 129 | 171 |
| *Y* | 16.60 | 16.60 | 17.80 | 35.00 | 16.90 | 16.90 | 26.50 | 18.90 | 19.90 | 19.00 | 21.40 | 20.80 | | | | 22.70 | 23.8 |
| *Th* | 5.79 | 5.64 | 5.74 | 8.40 | 0.82 | 0.82 | 2.36 | 1.95 | 1.77 | 1.86 | 1.45 | 1.46 | | | | 7.65 | 9.56 |
| *U* | 1.01 | 0.95 | 0.80 | 2.40 | 0.19 | 0.20 | 0.56 | 0.46 | 0.42 | 0.43 | 0.36 | 0.38 | | | | 1.62 | 1.92 |
| Ta | 1.15 | 1.00 | 0.89 | 0.30 | 0.13 | 1.23 | 0.33 | 0.25 | 0.24 | 0.24 | 0.24 | 0.23 | | | | 0.78 | 0.83 |
| Hf | 1.70 | 1.90 | 1.80 | 4.20 | 0.13 | 1.23 | 3.02 | 2.22 | 2.18 | 2.16 | 2.52 | 2.53 | | | | 3.50 | 4.70 |
| *Zr/Y* | *3.21* | *3.51* | *3.33* | *4.06* | *2.72* | 2.75 | 4.72 | 4.83 | 4.34 | 4.52 | 4.73 | 4.90 | | | | 5.68 | 7.18 |
| *Zr/Nb* | 19.04 | 21.56 | 22.77 | *28.4* | 25.56 | 21.14 | 25.51 | 26.82 | 24.69 | 26.03 | 28.14 | 29.14 | | | | 23.45 | 23.42 |
| *K/Rb* | 620.3 | 561.1 | 597.4 | | | | | | | | | | | | | 605.93 | 557.0 |
| *K/Ba* | 25.74 | 21.60 | 23.92 | | | | | | | | | | | | | 37.63 | 21.71 |
| *Rb/Sr* | 0.043 | 0.037 | 0.039 | 0.18 | 0.04 | 0.04 | 0.07 | 0.07 | 0.06 | 0.07 | 0.05 | 0.04 | | | | 0.05 | 0.05 |
| *Rb/Ba* | 0.04 | 0.039 | 0.04 | 0.11 | 0.09 | 0.09 | 0.10 | 0.01 | 0.09 | 0.10 | 0.08 | 0.07 | | | | 0.06 | 0.04 |

Table 1. Continued....

| | **Olivine Basalt of Merbabu Volcano** | | | **Tholeiitic Basalt of Karang-sambung (Anshori, 2007)** | **Tholeiitic Basalt of Galunggung Volcano Demsey, 2013)** | | **Basaltic Andesite of Galunggung Volcano (Demsey, 2013)** | | | | | | **Basaltic Andesite of Merbabu Volcano** | | | | |
|---|---|---|---|---|---|---|---|---|---|---|---|---|---|---|---|---|---|
| | **SRI-0328** | **SRI-0322** | **SRI-0332** | **River Medana** | **Gal 132a** | **Gal 132b** | **Gal 133** | **Gal 134** | **Gal 135** | **Gal 136** | **Gal 137a** | **Gal 137b** | **SRI-0221** | **SRI-0222** | **SRI-0233** | **SRI-0336** | **SRI-0334** |
| *Rare Earth Elements* | | | | | | | | | | | | | | | | | |
| *La* | 12.10 | 12.10 | 3.00 | 19.60 | 4.03 | 4.12 | 9.65 | 8.29 | 7.85 | 7.99 | 6.55 | 6.64 | | | | 46.10 | 46.60 |
| *Ce* | 24.90 | 25.00 | 25.80 | 43.80 | 9.60 | 9.65 | 21.83 | 17.88 | 17.16 | 17.25 | 15.22 | 15.55 | | | | 21.30 | 20.40 |
| *Pr* | 2.90 | 2.94 | 3.05 | 5.28 | 1.49 | 1.49 | 3.20 | 2.50 | 2.43 | 2.44 | 2.31 | 2.35 | | | | 5.23 | 5.25 |
| *Nd* | 12.40 | 12.40 | 13.00 | 23.00 | 7.15 | 7.16 | 14.68 | 11.0 | 10.86 | 10.61 | 10.76 | 10.89 | | | | 21.40 | 21.10 |
| *Sm* | 3.10 | 3.10 | 3.20 | 5.30 | 2.05 | 2.05 | 3.63 | 2.64 | 2.73 | 2.71 | 2.82 | 2.85 | | | | 4.70 | 4.60 |
| *Eu* | 0.90 | 0.90 | 1.00 | 1.47 | 0.78 | 0.80 | 1.19 | 0.92 | 1.00 | 0.92 | 0.96 | 0.97 | | | | 1.30 | 1.30 |
| *Gd* | 3.70 | 3.50 | 3.70 | 6.20 | 2.71 | 2.75 | 4.41 | 3.28 | 3.30 | 3.20 | 3.52 | 3.53 | | | | 5.00 | 5.00 |
| *Tb* | 0.46 | 0.45 | 0.47 | 1.00 | 0.45 | 0.45 | 0.70 | 0.52 | 0.53 | 0.53 | 0.57 | 0.56 | | | | 0.62 | 0.66 |
| *Dy* | 3.10 | 3.00 | 3.20 | 5.70 | 2.69 | 2.72 | 4.19 | 2.97 | 3.10 | 3.04 | 3.30 | 3.37 | | | | 4.10 | 4.30 |
| *Ho* | 0.60 | 0.60 | 0.60 | 1.10 | 0.55 | 0.54 | 0.87 | 0.60 | 0.63 | 0.61 | 0.68 | 0.71 | | | | 0.80 | 0.80 |
| *Er* | 1.70 | 1.70 | 1.80 | 3.60 | 1.61 | 1.62 | 2.52 | 1.80 | 1.89 | 1.81 | 1.97 | 1.98 | | | | 2.40 | 2.60 |
| *Tm* | 0.20 | 0.20 | 0.20 | 0.54 | 0.25 | 0.25 | 0.41 | 0.29 | 0.29 | 0.29 | 0.31 | 0.32 | | | | 0.30 | 0.40 |
| *Yb* | 1.70 | 1.60 | 1.70 | 3.30 | | | | | | | | | | | | 2.30 | 2.70 |
| *Lu* | 0.24 | 0.25 | 0.26 | 0.48 | 0.26 | 0.26 | 0.41 | 0.31 | 0.33 | 0.32 | 0.33 | 0.34 | | | | 0.36 | 0.41 |
| *∑REE* | 68 | 67.74 | 70.98 | 120.37 | 33.62 | 33.86 | 67.69 | 53 | 52.1 | 51.72 | 49.3 | 50.06 | | | | 115.91 | 116.1 |
| *TRE* | 84.60 | 84.34 | 88.78 | | 52.10 | 52.33 | 96.71 | 73.74 | 73.98 | 72.57 | 72.70 | 72.88 | | | | 138.61 | 139.9 |
| *TREO* | 95.10 | 94.82 | 99.83 | 174.94 | 58.95 | 59.21 | 109.15 | 83.15 | 83.48 | 81.86 | 82.14 | 82.30 | | | | 155.57 | 157.1 |
| *TRExOy* | 101.89 | 101.61 | 106.96 | 187.45 | 62.99 | 63.26 | 116.76 | 88.99 | 89.31 | 87.59 | 87.83 | 88.00 | | | | 166.90 | 168.6 |
| $TRE_2O_3$ | 100.35 | 100.05 | 105.35 | 184.73 | 62.38 | 62.64 | 115.37 | 87.86 | 88.23 | 86.50 | 86.86 | 87.01 | | | | 164.05 | 65.67 |

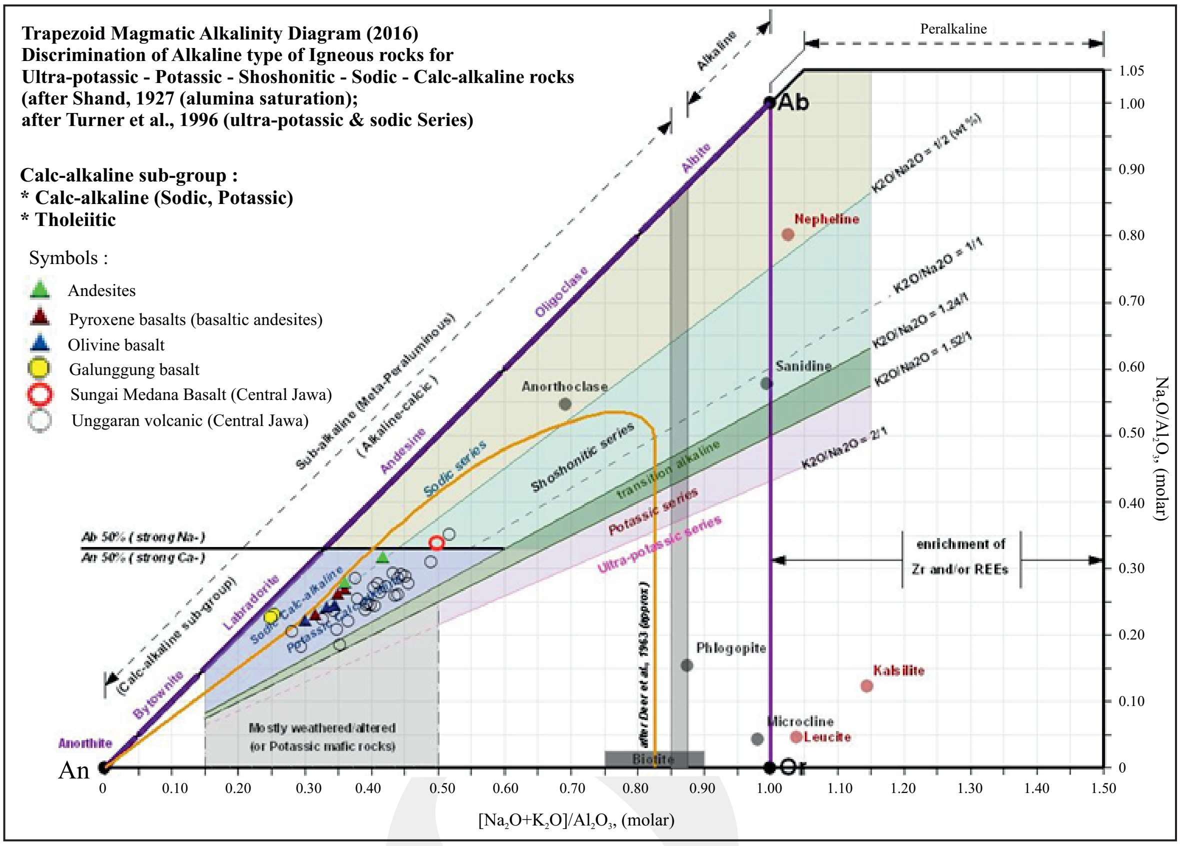


Figure 9. Trapezoid diagram shows potassic calc-alkaline series correlate negatively with $SiO_2$ pointing to fractionation signature or cogenetic relationship.

Merbabu volcanic rocks. This is the opposite to the tholeiitic basalt of Medana River (Anshori, 2007) and Galunggung Volcano (Demsey, 2013), as well as olivine basalt of Merbabu Volcano.

## Trace and Rare Earth Elements

Trace and rare earth elements on Merbabu volcanic rocks can be divided into two groups, *i.e.* compatible elements and incompatible elements. The compatible elements in basalt are characterized by the enrichment in Ba and Sr, but low in Cr, Ni, and Cu. Compared to tholeiitic basalt of Medana River, this basalt contains Ba and Sr ~500 ppm, Zr ~55 ppm.

Compatible elements of Merbabu basalt contain Cr of 28 - 37 ppm, Ni of 21 - 27 ppm, and Sc of 24 - 25 ppm. Tholeiitic basalt of Galunggung Volcano has very high Cr (~521 ppm), high Ni (~160 ppm), and high Sc (~39 ppm) (Dempsey, 2013). While tholeiitic basalt of Medana River contains Cr (<20 ppm), high Ni (<20 ppm), and high Sc (~28 ppm) (Anshori, 2007). This can be interpreted that Merbabu basalt is more enriched than tholeiitic volcanic basalt of Galunggung and less enriched than Medana River.

Incompatible elements of Merbabu basalt shows high-medium K (~14,000 ppm), medium Nb (~2.75 ppm), and higher Rb (>23 ppm). While Galunggung basalt has Rb (7.5 ppm), Y (~17 ppm), and Th (~0.82 ppm); and Medana River has Th of 8.40 ppm. In Merbabu basalt, La contents vary considerably (12.1−13.0 ppm), whereas Yb contents range from 1.6 to 1.7 ppm resulting in La/Yb ratios of 7.117–7.647. Major and trace element bivariate plots for $Fe_2O_3$, MgO, CaO, and Ni are presented in Figure 10.

Both the olivine-rich basalt and basalt do not show any major trends, most likely due to the small number of samples and their restricted range in $SiO_2$ content. The rocks display mod-

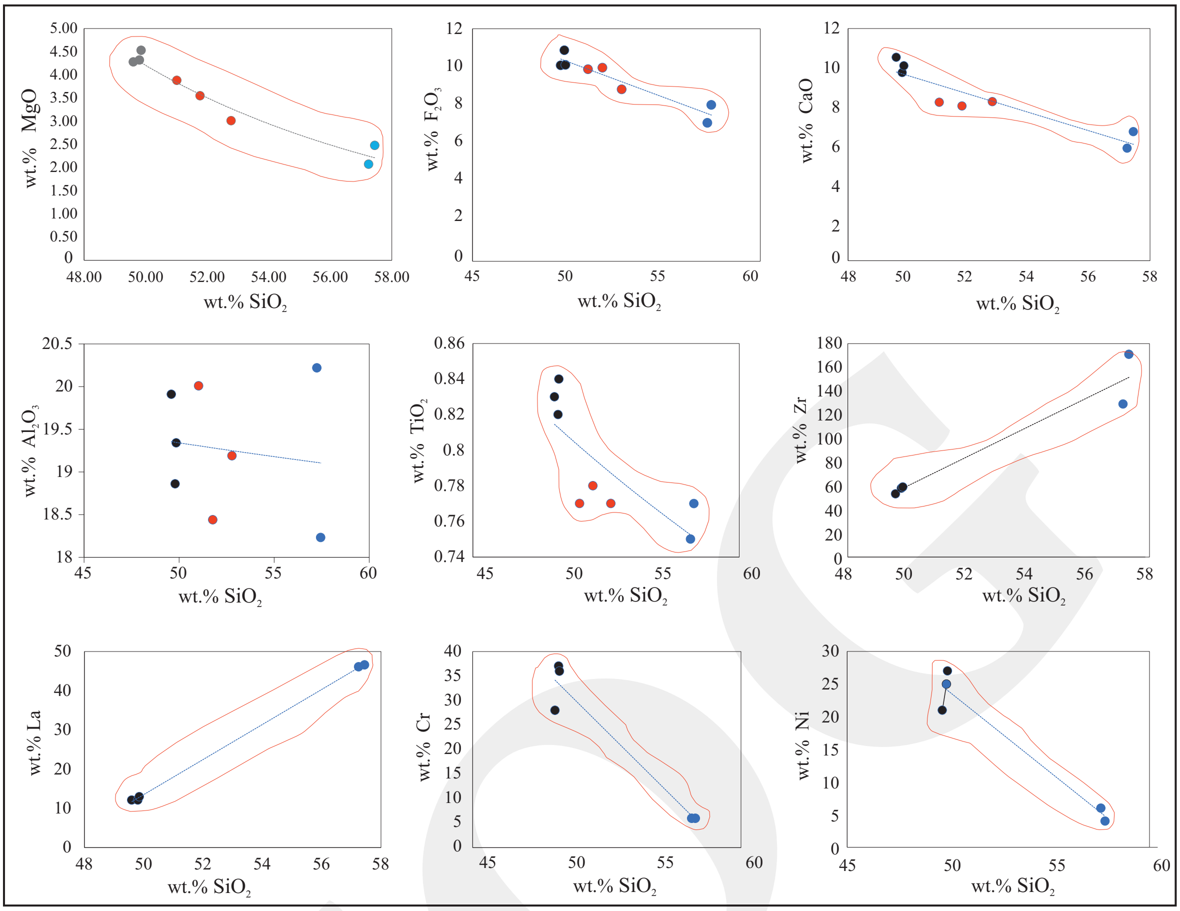


Figure 10. Major and trace element variation diagram for the Merbabu volcanic rocks exposed on the tracks of Thekelan and Kajor; symbol shown in Figure 9.

erately enriched-LREE (Figure 11). The olivine basalt and basaltic andesite (Figure 12) display enrichment in Rb, Ce,U, K, and Pb relative to the less compatible elements (with flatter multielement patterns $(Nb/La)_{pm}$= ~0.6-1) and Ti anomalies, where PM refers to primitive mantle normalized values (Ti/La= 0.005 - 0.006).

## Discussion

In a magmatic equilibrium system, magma is composed of minerals, silicate melt, and gases with compatible and incompatible elements that formed during their crystalization. The compatible elements are particularly partitioned into solid phases, and the incompatible elements into melt phases (Winchester and Floyd, 1977). In the beginning, the Merbabu Volcano produced basaltic materials about 40 ka. As mentioned above, thin section and major element analyses inform that basalts and basaltic andesites composed the southern flank (older) of Merbabu Volcano. It means during its activity, this volcano had erupted in different kind with different volcanic materials, starting from olivine-rich basalt, basalt, and andesite. Magmatism below Merbabu Volcano has evolved, implied to the frequency and the intensity of the volcanic activity.

Normalized variation diagram with Normal Mid-Oceanic Ridge Basalt (N-MORB) *versus* subduction-related magmas (adobted from McCulloch and Gamble, 1991; Elliot *et al*., 1997; Turner and Hawkesworth, 1997; and Handley *et al*., 2007) has highlighted the enrichments of the fluid mobile elements (LILE and LREE) over the less mobile elements (HFSE and HREE) of Merbabu volcanic basalt and their comparations

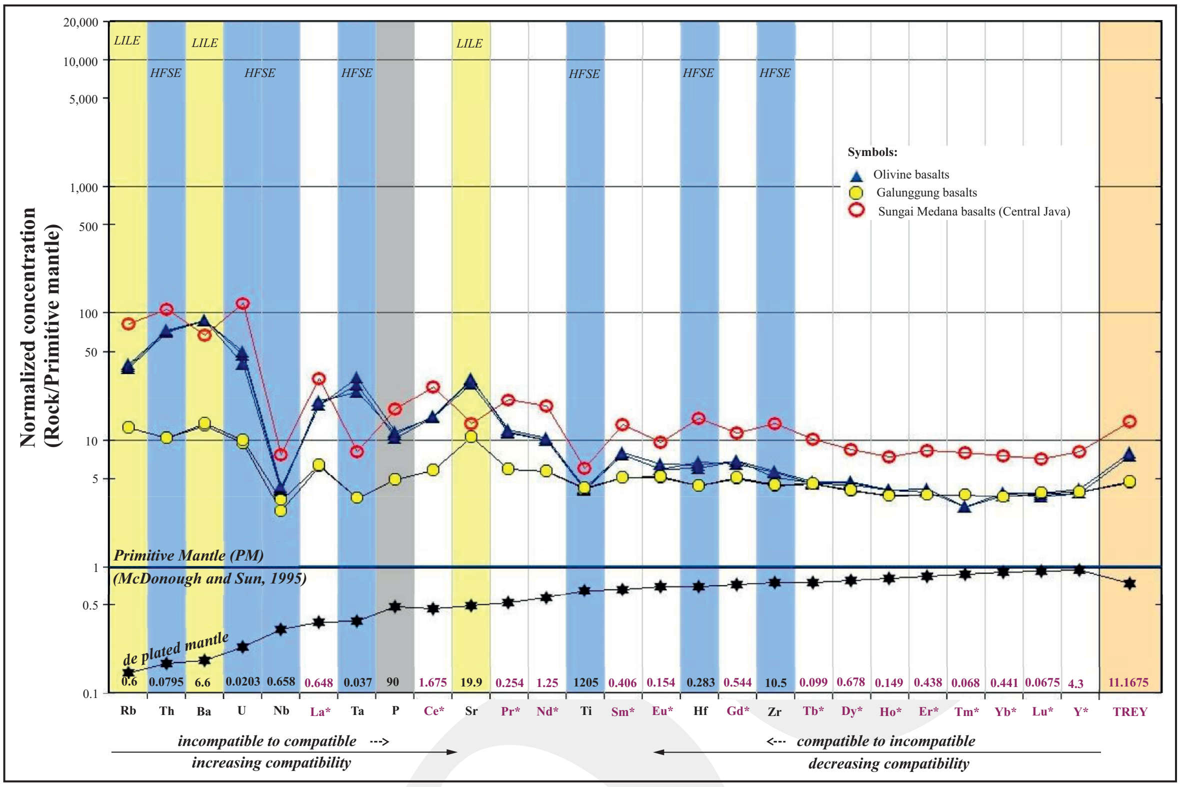


Figure 11. Chondrite normalized REE diagrams for Merbabu basalt compared to tholeiitic basalt of Medana River and Galunggung Volcano (after Sun and McDonough, 1989).

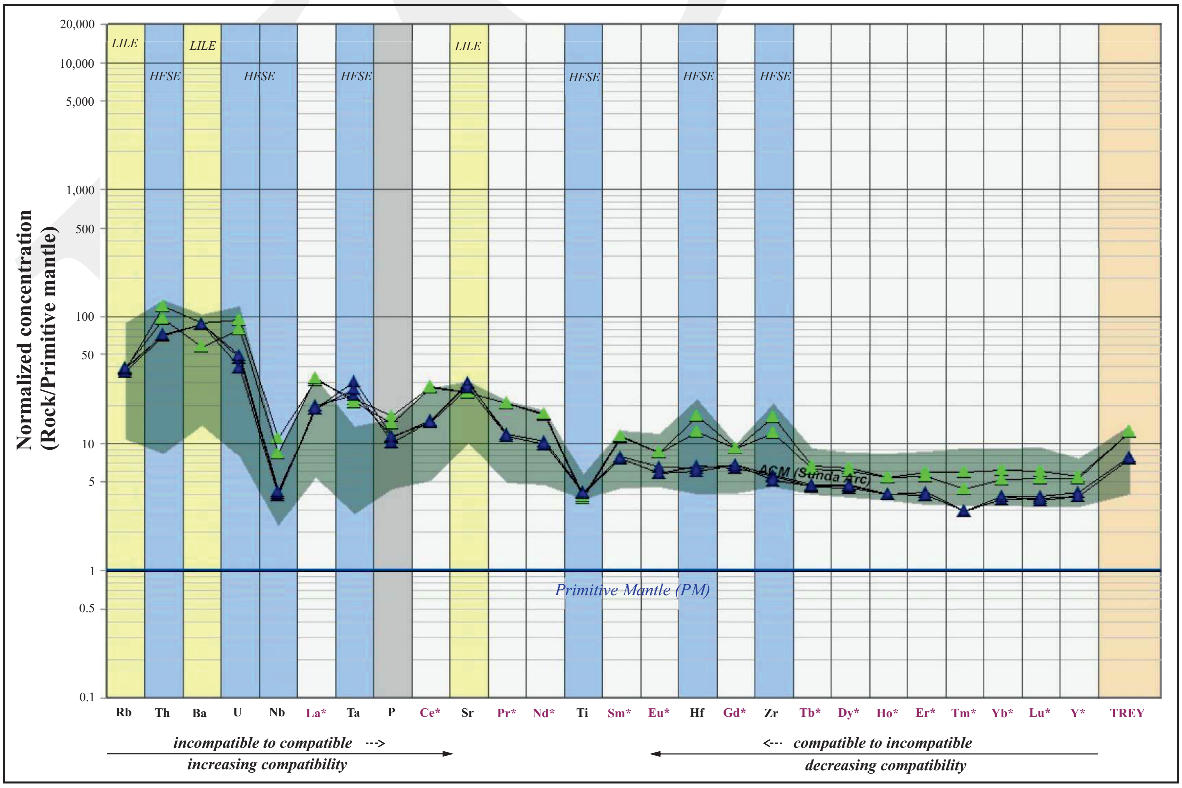


Figure 12. Chondrite normalized REE diagram for Merbabu olivine-rich basalt and basaltic andesite (after Sun and Mc-Donough, 1989).

of the tholeiitic basalt of Medana River (Karangsambung, Central Java) and the tholeiitic volcanic basalt of Galunggung Volcano (West Java) (Table 1 and Figure 11). This shows that HFSE and HREE concentrations of Merbabu olivine-rich basalt tend to transitional to tholeiitic magma. This is shown by the similar pattern of both spider diagram and the REE normalized diagram adopted from McDonough and Sun (1995) for both olivine-rich basalt and basalt (Figure 12). According to Woodhead *et al*. (1993), based on the abundancy of the incompatible elements compared to the compatible elements, it is known that the olivine basalt has increasing incompatibility, which means an enrich-mantle source. It can be inferred to the presubduction mantle source.

Theoritically, oceanic basalts are uncontaminated by continental crust, therefore their compositions should be ilustrating their respective mantle sources. On the other hand, mid-oceanic-ridge basalts (MORBs) provide the upper depleted mantle characterization, while oceanic intraplate basalts (OIBs) provide the lower mantle (as primitive magma). As said by Hamilton (1979) above, Merbabu Volcano has been formed as the constituent of the volcanic arc produced by the subducting system of Indian-Australian Oceanic Plate below the Eurasian Plate. As none to MORB nor OIB, tholeiitic basalt originated from subducting plate boundary should be alkaline, and might enrich mantle source of incompatible elements. The ratios of incompatible elements in order to distinguish the source reservoirs; the K/Ba ratio is as high as 21−25.74, suggesting as parental oceanic island alkaline *basalt* (OIAs).

As the depleted mantle source, the MORB (I-MORB) sample has commonly inferred to have slightly more "enriched" source (Gertisser and Keller, 2003; Handley *et al*., 2010). It means that the HZR has a similar profile to the LZR with very slight enrichments in Th, Ba, Nb, Sr, Ta, and Zr, an increase of Lu to Cs concentrations. It also has some large positive anomalies for Sr, Pb, K, and Ba, but negative anomalies for Nb and Ta. Most of the HFSE and HREE in the Merbabu basalt are higher in concentration than N-MORB. These are characterized by the enrichments in Th, Ba, U, La, Ta, and Sr, with negative anomalies for Nb, Ti, Sm, Eu, Hf, Gd, Zr, and Tm concentrations.

Chondrite normalizes REE plots (Figure 11) compared to the tholeiitic basalt lava of Galunggung Volcano and Medana River. It is shown that basalt of Merbabu magma has low-Zr such as Galunggung magma, but none to Medana River magma. In the low Zr of basaltic group, it shows greater enrichment in LREE (~ 35 times Chondrite) and slightly higher HREE (~15 times Chondrite) than the basaltic-andesite. The high Zr shows similar REE trends to the low-Zr group. This andesite contains a great amount of LREE (~45 times Chondrite) and low Zr compositions. It is similar to the andesitic volcanic rocks of Merbabu Volcano compared to Sumbing Volcano occuring in the concentrations of Pr, Nd, Sm, Eu, Gd, Tb, and Dy. Merbabu volcanic rocks have higher concentrations of La and Yb, but lower concentration of Ce.

Compared to N-MORB, the Kelut samples display lower, slightly concave up, MREE to HREE; and higher LREE. However, they show ubiquitously lower REE than all of the other medium- to high-K volcanic-arc rocks from East Java which contain up to a hundred times Chondrite LREE and twenty-five times Chondrite HREE. The leucititic volcanic rocks have between two hundred and seven hundred times Chondrite LREE and as low as five times Chondrite HREE.

The olivine basalt of Merbabu Volcanic rocks is rich in olivine and clinopyroxene. Theoretically, the elements of Sc, Cr, Co, and Ni in magma show compatible phases of silicate melt where Sc is compatible in clinopyroxene but not in olivine. Data show Sc in the range of 24−25 ppm in olivine basalt, but 10−13 ppm in basaltic andesite. It can be interpreted that the Sc contents in the olivine basalt of the track in Kajor are preferentially partitioned into silicate melts rather than coexisting minerals.

Petrologically, the basaltic andesite has less olivines but more clinopyroxenes which is consistent to the higher contents of CaO. Ca in augite-aegirine functions as decreasing pressure and temperature during the crystallization, thus it is usable to reconstruct the solid solution (Smith and Lindsley, 1971; Ballaran *et al.* 2015). The higher content of Zr and P in basaltic andesite than in olivine basalt, indicates that Zr is compatible in zircon and P is compatible in apatite but neither in olivine nor pyroxene. The basaltic andesite shows fractionated patterns as shown by La/Yb ratios of 17 - 20 which is lower than adakites (La/Yb = 40; Sun and McDonough, 1989), and interpreted as garnet ± amphibole source indication in partial melting (Figure 13). The data correlate with the discriminants for mantle melting array *versus* arc basalt, that explains the basaltic andesite is originated from the partial melting of the active continental margin, while the olivine basalt is from a transitional enriched mantle.

The increasing Zr content from 53 - 59 in olivine basalt into 129 - 171 in basaltic andesite, according to Pearce and Peate (1995) signifies the involvement of both slab melt and hydrous fluid in the source rocks, which is out of the MORB. The involvement of slab partial melts in the petrogenesis of the olivine basalt and the basaltic andesite suggests that temperature in the subduction zone was suffciently high to initiate partial melting of the slab, possibly both of the oceanic plate and the continental plate. This is also shown by the presence of the enrichment of the mantle source in the HFSE (Figure 12), that has been sourced from the subducting oceanic slab. Figure 14 of the tectonic discrimination diagram Ta/Hf and

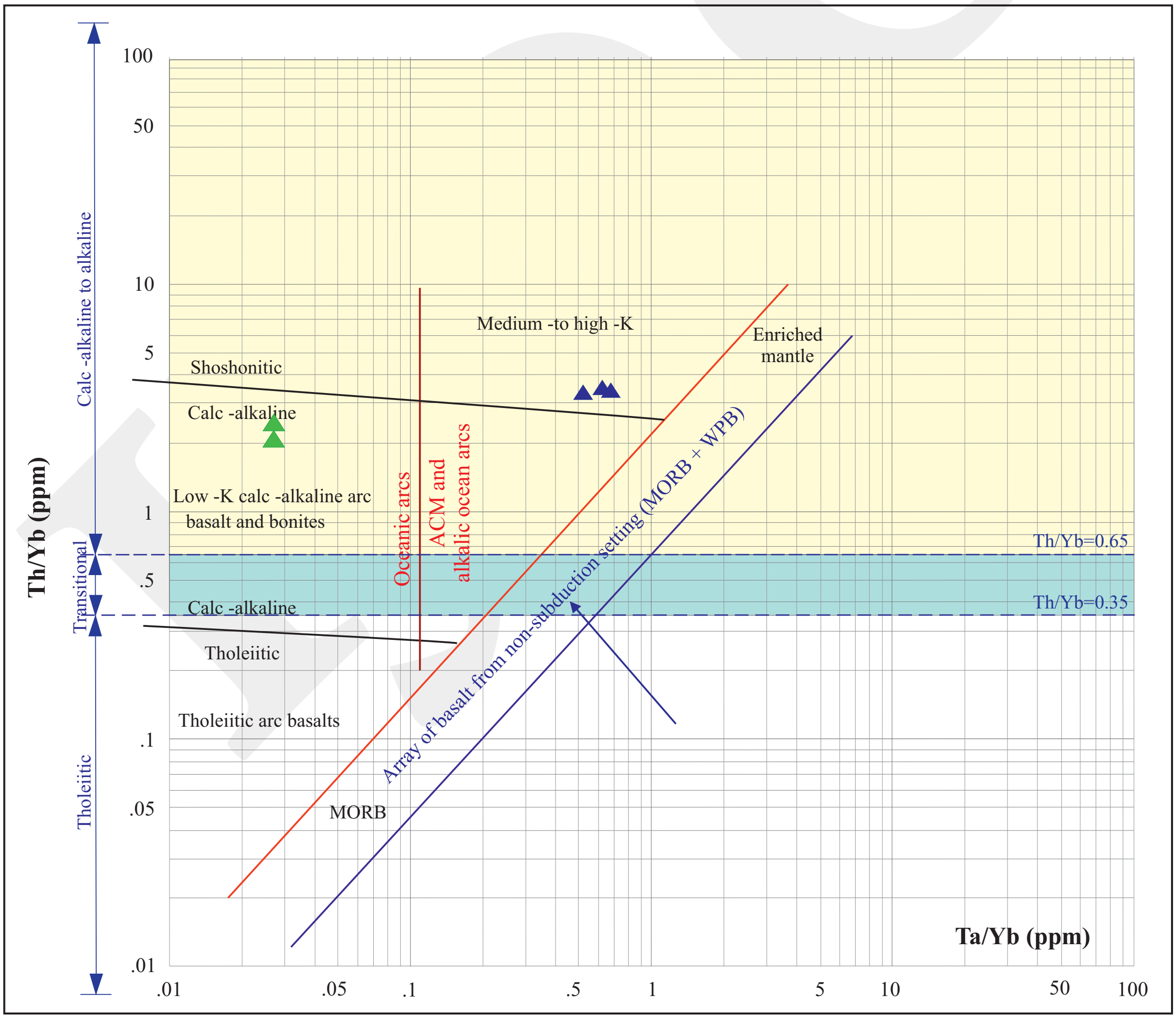


Fugure 13. Diagram plots of Th/Yb (in ppm) and Ta/Yb (in ppm) explains medium to high K ACM originating magma series for olivin basalt (blue) and Calc-alkalline magma series for andesite (green) (diagram: after Pearce, 2008 and MacLean and Barrett, 1993).

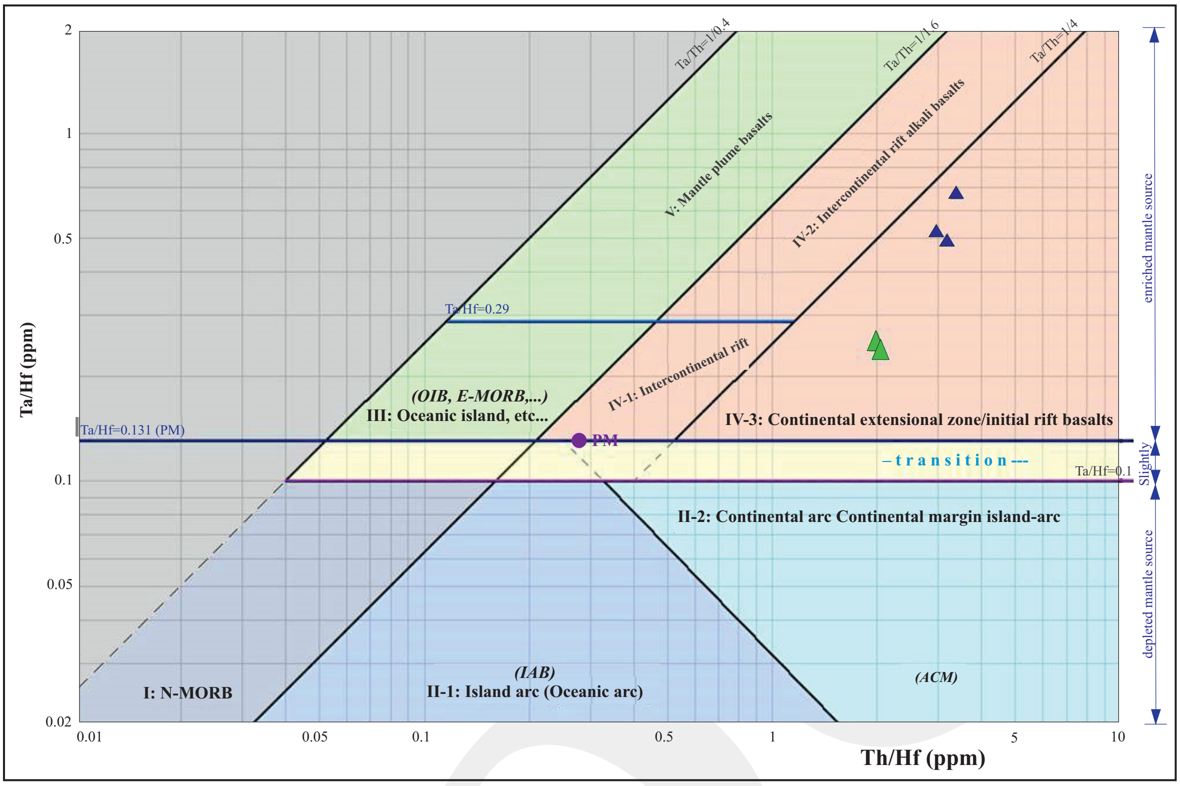


Figure 14. Diagram plot Ta/Hf (wt ppm) and Th/Hf (wt ppm) shows tectonic setting of the magmatic origin for olivine basalt (blue), *i.e.* continental extentional zone (initial rift basalt?) (after Wang *et al*., 2001).

Th/Hf is particularly explaining that the enrichment in the HFSE is relative to the continental extensional zone.

## Conclusion

The Merbabu volcanic rocks exposed at the tracks of Kajor-Selo consist of olivine basalt and basaltic andesite. Both are covered by andesite. The olivine basalt has slightly flat REE patterns and enriched by incompatible elements, while basaltic andesite has more enriched-LREE. Trace element systematics of the olivine basalt and basaltic andesite are characterized by fractionated REE patterns, enrichment of the HFSE relative to NMORB, and have slight anomalies of Nb and Ta. Therefore, this is consistent with derivation of these rocks by partial melting of a mantle wedge that suggests it was formed by shallow partial melting in a convergent tectonic setting. The $TiO_2$, $P_2O_5$, Zr, and overall lower abundance of total REE compared to the tholeiitic basalts of Medana River and Galunggung Volcano, the Eu, Sr, and Ti have slight anomalies in extended trace element spidergrams which is in a shallow level fractional crystallization. The close spatial association of the three petrological types in the Merbabu volcanic rocks is interpreted as reflecting their formation in an evolving oceanic arc into continental active margin enriched-LREE in continental rift basalts.

## Acknowledgments

Many thanks are addressed to Department of Geological Engineering- FTM of IST AKPRIND Yogyakarta for the legal permision, so this research can be finished along the hiking tracks of Kajor, Banyudono, and Thekelan. The geochemical and trace element analyses have been performed using ICP-MS method in The INTERTEK Global Mineral. Special thanks are due to Rui Alves Ximenes, Bekti Arif Rumanto, and Syarif Hidayat who helped in collecting samples in the field.

## References

Anonymous, 2013. *Geological Summary on Merbabu Volcano*. Global Volcanism Program, Smithsonian Institution.

Anshori, C., 2007. Petrogenesa Basalt Sungai Medana Karangsambung, Berdasarkan Analisis Geokimia. *Jurnal Riset Geologi & Pertambangan,* 17 (1), p.37-50. DOI:10.14203/risetgeotam2007.v17.143

Ballaran, T,B., Carpenter, M., Domeneghetti, M., and Tazzoli, V., 2015. Structural mechanisms of solid solution and cation ordering in augite-jadeite pyroxenes: I, A macroscopic perspective, *American Mineralogist*, 83 (5-6), p.419-433, DOI:10,2138/am-1998-5-601. DOI:10,2138/am-1998−5-601.

Ballaran, T.B., Uenver-Thiele, L., and Woodland, A.B., 2015. Complete substitution of $Fe^{2+}$ by Mg in $Fe_4O^5$: The crystal structure of the $Mg2Fe_2O^5$ end-member. *American Mineralogist*, 100 (2-3), p.628-632. DOI:10.2138/am-2015-5138

Bemmelen, R.W.van. 1949. *The geology of Indonesia, vol. IA,* General Geology. Martinus Nijhoff, The Hague. Netherlands, 732pp.

Dempsey, S.R., 2013. *Geochemistry of volcanic rocks from the Sunda Arc*, Durham University theses. http://etheses.dur.ac.uk/6948.

Elliott, T., Plank, T., Zindler, A., White, W.M., and Bourdon, B., 1997. Element transport from slab to volcanic front at the Mariana arc*, Journal of Geophysical Research,* 102, 14, p.991-15,019. DOI:10.1029/97jb00788

Gertisser, R. and Keller, J., 2003. Trace element and Sr, Nd, Pb, and O isotope variations in medium-K and high-K volcanic rocks from Merapi Volcano, Central Java, Indonesia: evidence for the involvement of subducted sediments in Sunda Arc magma genesis. *Journal of Petrology*, 44 (3), p.457-489. DOI:10.1093/petrology/44.3.457

Gomez, C., 2012. Multiscale topographic analysis of Merbabu and Merapi volcanoes using wavelet decomposition, *Environmental Earth Sciences*, 67 (5), p.1423-1430. DOI:10.1007/s12665-012-1587-1

Hamilton, W.B., 1979. *Tectonics of the Indonesian region.* US Government Printing Office.

Handley, H.K., Macpherson, C.G., Davidson, J.P., Berlo, K., and Lowry, D., 2007. Constraining fluid and sediment contributions to subduction-related magmatism in Indonesia: Ijen Volcanic Complex. *Journal of Petrology*, 48 (6), p.1155-1183. DOI:10.1093/petrology/egm013

Handley, H.K., Macpherson, C.G. and Davidson, J.P., 2010. Geochemical and Sr–O isotopic constraints on magmatic differentiation at Gede volcanic complex, west java, Indonesia. *Contributions to Mineralogy and Petrology*, 159 (6), p.885-908.

Le Bas, M.J., Rex, D.C., and Stillman, C.J., 1986. The early magmatic chronology of Fuerteventura, Canary Islands. *Geological Magazine*, 123 (3), p.287-298. DOI:10.1017/s0016756800034762

Le Roex, A.P., Dick, H.J.B., Erlank, A.J., Reid, A.M., Frey, F.A. and Hart, S.R., 1983. Geochemistry, mineralogy and petrogenesis of lavas erupted along the Southwest Indian Ridge between the Bouvet triple junction and 11 degrees east. *Journal of Petrology*, 24 (3), p.267-318.

Maitre, L., 1989. A classification of igneous rocks and glossary of terms. *Recommendations of the International Union of Geological Sciences Subcommission on the Systematics of Igneous Rocks*, 193. DOI:10.1017/s0016756803388028

Maitre, R.W. (ed.), 2002. Igneous Rocks. A Classification and Glossary of Terms. *Recommendations of the International Union of Geological Sciences Subcommission on the Systematics of Igneous Rocks, 2nd ed*. xvi + 236 pp. Cambridge, New York, Melbourne. DOI:10.1017/s0016756803388028

McCulloch, M.T. and Gamble, J.A., 1991. Geochemical and geodynamical constraints on subduction zone magmatism. *Earth and Plan-*

*etary Science Letters*, 102 (3-4), p.358-374. DOI:10.1016/0012-821x(91)90029-h

McDonough, W.F. and Sun, S.S., 1995. The composition of the Earth. *Chemical Geology*, 120 (3-4), p.223-253.

MacLean, W.H., and Barrett, T.J., 1993. Lithogeochemical technique using immobile elements. *Journal of Geochemical Exploration,* 48 (2), p.109-133.

Mulyaningsih, S., 2006. *Geologi lingkungan di daerah lereng selatan Gunung Api Merapi, pada waktu sejarah (Historical time)*. Disertation in Departemen Teknik Geologi, Sekolah Tinggi Pascasarjana Institut Teknologi Bandung. DOI:10.5614/bull.geol.2017.1.1.1

Mulyaningsih, S., Hidayat, S., Rumanto, B.A., and Saban, G., 2016. Identifikasi Karakteristik Erupsi Gunung Api Merbabu Berdasarkan Stratigrafi dan Mineralogi Batuan Gunung Api. *Prosiding Snast*, p.85-97.

Pearce, J. A., 2008. Geochemical fingerprinting of oceanic basalts with applications to ophiolite classification and the search for Archean oceanic crust. *Lithos,* 100, p.14-48.

Pearce, J.A. and Peate, D.W., 1995. Tectonic implications of the composition of volcanic arc magmas, *Annual Review of Earth & Planetary Sciences,* 23, p.251-285. DOI:10.1146/annurev.ea.23.050195.001343

Shand, S.J., 1927. On the relations between silica, alumina, and the bases in eruptive rocks, considered as a means of classification. *Geological Magazine*, 64 (10), p.446-449. DOI:10.1017/s0016756800103760

Smith, D. and Lindsley, D.H., 1971. Stable and metastable augite crystallization trends in a single basalt flow, *American Mineralogist*, 56 (1-2), 225pp.

Sun, S.S. and McDonough, W.F., 1989. Chemical and isotopic systematics of oceanic basalts: implications for mantle composition and processes. *Magmatism in The Ocean Basins*, p.313-345. DOI:10.1144/gsl.sp.1989.042.01.19

Turner, S., Arnaud, N., LIU, J., Rogers, N., Hawkesworth, C., Harris, N., Kelley, S., Van Calsteren, P. and Deng, W., 1996. Post-collision, shoshonitic volcanism on the Tibetan Plateau: implications for convective thinning of the lithosphere and the source of ocean island basalts. *Journal of Petrology*, 37 (1), p.45-71.

Turner, S. and Hawkesworth, C., 1997. Constraints on flux rates and mantle dynamics beneath island arcs from Tonga–Kermadec lava geochemistry. *Nature*, 389 (6651), p.568. DOI:10.1038/39257

Wang, Y.N., Zhang, C.J., and Xiu, S.Z., 2001. Th/Hf-Ta/Hf identification of tectonic setting of basalts. *Acta Petrol Sin* (in Chinese), 17(3), p.413-421.

Winchester, J.A. and Floyd, P.A., 1977. Geochemical discrimination of different magma series and their differentiation products using immobile elements, *Chemical Geology,* 20 (C), p.325-343. DOI:10.1016/0009-2541(77)90057-2

Woodhead, J., Eggins, S., and Gamble, J., 1993. High field strength and transition element systematics in island-arc and back-arc basin basalts: evidence for multiphase melt extraction and a depleted mantle wedge. *Earth and Planetary Science Letters*, *114* (4), p.491-504. DOI:10.1016/0012-821x(93)90078-n